Carbohydrate Polymer Technologies and Applications 7 (2024) 100436

Contents lists available at ScienceDirect

Carbohydrate Polymer Technologies and Applications

journal homepage: www.sciencedirect.com/journal/carbohydrate-polymer-technologies-and-applications

Rheological, thermal and spectroscopical properties of the macromolecular complex between sodium hyaluronate and cisplatin for anticancer chemotherapy

Sabrina Banella [a,b], Abu T.M. Serajuddin [b], Gaia Colombo [a,*], Marco Scoponi [c,d]

[a] Department of Life Sciences and Biotechnology, University of Ferrara, Via Fossato di Mortara 19, 44121 Ferrara, Italy
[b] Department of Pharmaceutical Sciences, St. John's University, 8000 Utopia Parkway, Queens, NY 11439, USA
[c] Institute for Organic Synthesis and Photoreactivity, Research National Council (ISOF-CNR), c/o University of Ferrara, Dept. of Life Sciences and Biotechnology, Via L. Borsari 46, 44121 Ferrara, Italy
[d] Advanced Polymer Materials Srl, Via Saragat 9, 44122 Ferrara, Italy

ARTICLE INFO

Keywords:
Loco-regional delivery
Sodium hyaluronate
Cisplatin
Complexation
Viscoelasticity
SEC
DSC

ABSTRACT

Hyaluronic acid and its sodium salt (sodium hyaluronate; hyaluronan; NaHA) are widely used for drug delivery. Here, a thin film of high molecular weight NaHA with the anticancer agent cisplatin (cisPt) was prepared to deliver the drug loco-regionally on the pleura after tumor resection. For preparing films, NaHA, cisPt, and excipients were dissolved in water; the resulting viscous film-forming mixture (FFM) was cast into wet films and dried. It was discovered that a cisPt/NaHA complexation in films was responsible for the observed higher drug efficacy from films. Here, we investigated the rheological, thermal and spectroscopical properties of the cisPt/NaHA complex. The size exclusion chromatography (SEC) showed a unimodal molecular weight distribution of NaHA in aqueous solution. The viscosity of FFM increased with increasing cisPt concentration, indicating cross-linking due to cisPt/NaHA complexation. In DSC analysis, the water evaporation temperature of both FFM and film decreased due to cisPt/NaHA complexation, suggesting that the complexation with Pt^{2+} displaced water molecules originally bound to NaHA. FTIR-ATR spectral changes in cisPt-loaded *vs.* placebo films suggested that complexation involved the carboxylate groups of the polysaccharide. Finally, energy dispersive spectroscopy coupled with SEM demonstrated that the cisPt/NaHA complex in films appeared to be a network of aggregates.

Introduction

Cisplatin (cisPt) is used for the chemotherapy of many solid tumors. Given by the intravenous (IV) route, the drug acts by cross-linking with purine bases of DNA, causing unrepairable DNA damage and, subsequently, apoptosis of cancer cells (Gold & Raja, 2021). However, because of the severe side effects of cisPt on liver and kidneys following IV injection, alternative polymer-based drug delivery systems have been investigated specifically targeting cancer cells by controlling the pharmacokinetics of the drug, notably its distribution and excretion (Dasari & Tchounwou, 2014; Davoudi et al., 2022; Gold & Raja, 2021; Moura et al., 2019; Wen et al., 2018). For example, Nishiyama et al. (2001) studied cisplatin-loaded micelles made of poly(ethylene glycol)-poly (aspartic acid) block copolymer that accumulated preferentially at tumor sites and reduced nephrotoxicity. In addition, polymeric carriers may reduce cell resistance to anticancer drugs, including cisPt (Boztepe et al., 2021).

The polysaccharide polymer hyaluronic acid (HA) or its sodium salt, sodium hyaluronate (NaHA) or hyaluronan (Fig. 1), are widely used as polymeric carrier for drug delivery (Talebian et al., 2018) because of their favorable properties like relatively high water solubility, viscoelasticity, biocompatibility, non-immunogenicity, biodegradability, and high affinity for CD44 receptor overexpressed by cancer cells (Chai et al., 2020; Mirzaei et al., 2023; Saravanakumar et al., 2014).

One particular example of an innovative delivery system containing sodium hyaluronate as the drug carrier is a dry thin film loaded with cisPt used for the loco-regional therapy of cancer. The film is stuck locally onto the mesothelium during surgery for resection of primary malignant pleural mesothelioma (Ampollini et al., 2010; Sonvico et al., 2018). Such intrapleural application of the film for cisPt release on site,

* Corresponding author at: Department of Life Sciences and Biotechnology, University of Ferrara, Via Fossato di Mortara 19, 44121 Ferrara, Italy.
E-mail address: clmgai@unife.it (G. Colombo).

https://doi.org/10.1016/j.carpta.2024.100436

Available online 17 January 2024

kills residual cancer cells and limits recurrences of cancer, as demonstrated in a pleural mesothelioma rat model (Ampollini et al., 2010). In an *in vivo* pharmacokinetic study using a healthy ovine model, the application of the cisPt-loaded hyaluronate film demonstrated prolonged and higher plasma drug (platinum) concentrations compared to intrapleural and intravenous administration of a cisPt solution. Interestingly, such high plasma levels of cisPt from the film were not associated with any increased toxicity on various organs like liver, kidneys, and heart. This evidence led to the hypothesis that cisPt circulated in the blood as a complex bound with hyaluronan (Ampollini et al., 2018). Recently, an *in vitro* study on 2D cell models of various tumors assessed the cytotoxicity of the cisPt/NaHA complex in solution as compared to the drug alone (Banella et al., 2023). The complex retained the drug activity and reduced the viability of pancreatic, melanoma, and lung cell lines in a concentration- and time-dependent manner. Indeed, the complexation of cisPt with unmodified NaHA is not new in the literature as several researchers exploited it to obtain nanoconjugates showing higher antitumor efficacy and lower toxicity compared to free cisplatin (Cai et al., 2008; Ishiguro et al., 2016; Tsai et al., 2013; Xie et al., 2010). However, none of these studies has characterized the cisPt/NaHA complex itself because they all focus on its activity *in vivo*. The existence of the complex is claimed by these authors based on the formation of particles in the nanometer size range suitable for lymphatic uptake after administration by injection or inhalation. Moreover, researchers at the University of Tokyo have synthesized chelating ligand-modified hyaluronans where cisPt binds to the ligand instead of the polymer backbone (Amano et al., 2022; Ohta et al., 2016, 2017). They have described the cross-linking of the hyaluronan derivative based on chain bridging or hydrophobic interactions, but did not demonstrate it.

In light of the above, a thorough understanding of the chemical nature and physicochemical properties of cisPt/NaHA complex is necessary also to explain its activity at the biological level. In particular, no one has yet experimentally determined what functional groups of the polymer are involved in the interaction between cisPt and NaHA. Most of the reported literature brings in the carboxylate groups either of unmodified or derivatized hyaluronan. For example, Xie et al. (2010) mentioned that cisPt was conjugated via ester bonds between Pt^{2+} and the carboxylate groups of hyaluronan; however, no evidence of such bonds was given in the report. Normally, an ester is a compound where a covalent link is formed by reaction of an alcohol (hydroxyl group) with a carboxylic acid with the loss of a water molecule. The bond must be cleaved by chemical or enzymatic hydrolysis to release the drug for action. In a first work, our group searched for the complex between cisPt and NaHA in the dry film as well as in the liquid film-forming mixture (FFM) from which the film is manufactured (Banella et al., 2021). In both systems, the complex formation was demonstrated by indirect methods like (a) chromatographic determination of free (unbound) cisPt in the FFM and (b) quantification of cisPt in solution after release from the film *in vitro*. The same study clarified that the cisPt/NaHA complex controlled the release of cisPt from the film in 0.9 % NaCl solution even beyond the time required for the film to completely dissolve (Banella et al., 2021). These studies, however, lacked a direct determination of the complex and did not allow to confirm which functional groups of the NaHA polymer bind with platinum. The group acting as ligand must form coordination bonds with platinum (transition metal) by donating one or more electron pairs (Cotton et al., 1999; Kostova, 2006).

The objective of the present work was to characterize the interaction between cisPt and NaHA in aqueous colloidal dispersions and in the film. The hypothesis has been that the cisPt/NaHA complexation modifies spectroscopical and physicochemical properties of the polysaccharide and drug. Preliminarily, a thorough characterization of the structure of the high molecular weight hyaluronan (NaHA) polymer used for manufacturing the film was carried out. The mean molecular weight of the polymer was also confirmed. Then, the complexation between cisPt and NaHA was followed in aqueous solution by UV-Vis spectroscopy. The possible effect of the complexation on the viscoelasticity of NaHA was investigated by rheological measurements on NaHA solutions in water without and with cisPt at increasing concentrations. The novelty of the work is the gained knowledge about the cisPt/NaHA complex, which is the active element of several delivery systems for anticancer therapy with cisplatin. The study is important because the structure and stability of the complex influence the pharmacokinetics of cisPt, particularly its distribution throughout the body as well as its availability at tumor site, and ultimately its efficacy and safety.

Material and methods

Material

A high molecular weight (HMW) sodium hyaluronate (NaHA) or hyaluronan with a molecular weight >1 million Dalton was used in the present investigation as it was the one chosen for manufacturing the film. It was a kind gift by Fidia Farmaceutici S.p.A. (Abano Terme, PD, Italy; batch #A19270). The HMW hyaluronan was used for all experiments except the determination of cisPt-hyaluronan interaction by UV-Vis spectroscopy, where a low molecular weight (LMW) hyaluronan (76 kDa; batch #1908100435, VIVATIS PHARMA GmbH, Hamburg, Germany) was used. The HMW hyaluronan was substituted with the LMW hyaluronan because the aqueous solution of HMW hyaluronan was highly viscous *per se* and even more in presence of cisPt and, therefore, not suitable for spectrophotometric analysis. Cisplatin (cisPt) with a purity higher than 99.9 % was purchased from Sigma Aldrich (Saint Louis, MO, USA). Polyvinyl alcohol was obtained from Nippon-Goshei (PVA 83,400 Da, 87 % hydrolysis degree; Osaka, Japan). Polyethylene glycol 1000 monostearate (PEG 1000S) was a kind gift of CRODA (batch 0001459543; Snaith, UK). Polyethylene glycol 200 (PEG 200) and sorbitol were purchased from ACEF (Fiorenzuola d'Arda, PC, Italy). Water used for all preparations was Milli-Q ultrapure water (18 MΩ cm, Milli-Q system, Waters Corp., Milford, MA, USA). All other chemicals, reagents and solvents were of analytical grade.

Thermogravimetric analysis (TGA) of NaHA

TGA was performed using a Hi-Res modulated TGA Q500

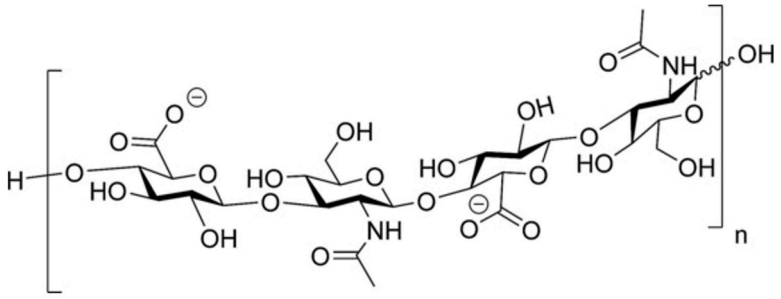

Fig. 1. Chemical structure of hyaluronate.

thermogravimetric analyzer (TA Instruments, New Castle, DE, USA). A sample of HMW hyaluronan weighing about 20 mg was placed in a platinum pan and heated from 35° to 900 °C under a continuous flow (70 ml/min) of dry nitrogen up to 600 °C, and then oxygen to 900 °C to collect ashes. Heating rate was automatically controlled so that heating progressed by 10 °C/min in the temperature range where the weight loss was less than 2 % (w/w). Conversely, when the weight loss was greater than 2 %, the heating rate was reduced at 2 °C/min.

Molecular weight distribution of HMW NaHA by size exclusion chromatography with triple detection (SEC-TD)

The size exclusion chromatography (SEC) apparatus consisted of a high-performance liquid chromatography pump unit (Knauer K501; KNAUER Wissenschaftliche Geräte GmbH, Berlin, Germany), a Rheodyne® valve (mod. 7725 J) for manual injection with a loop of 50 µl (IDEX, Lake Forest, IL, USA). The stationary phase was the TSK-GEL GMPWXL column (Tosoh Bioscience; Griesheim, Germany). The elution of an aqueous solution (pH 7.0) containing 0.1–0.15 M $NaNO_3$ and 0.05 % (w/v) sodium azide (antimicrobial agent) was carried out at a flow rate of 0.6 ml/min at 35 °C. The eluent was monitored by a refractive index detector (RI) (Knauer Smartline RI 2300; KNAUER Wissenschaftliche Geräte GmbH, Berlin, Germany) and Viscoteck system (mod TD270; Malvern Panalytical, Malvern, London, UK), which comprises a light-scattering detector at 7° (Low Angle Light Scattering, LALS) and 90° (Right Angle Light Scattering, RALS) angles and a differential viscosimeter. The chromatographic signals were analyzed on a computer workstation by means of the dedicated Omnisec v4.6 software.

The specific refractive index increment (dn/dc) was measured by using HMW NaHA solutions in water in the 0.15 to 0.40 mg/ml range at the 658 nm wavelength of RI detector. The expression dn/dc denotes the variation in refractive index (dn) of a solution as a function of its solute concentration (dc). All experiments were performed in triplicate.

Analysis of cisplatin complexation with sodium hyaluronate in solution by UV–Vis spectroscopy

An aqueous solution was prepared containing 0.066 % (w/v) cisPt and 2.5 % (w/v) low molecular weight (LMW) sodium hyaluronate (NaHA) such that the molar ratio between cisPt and the repeating unit of NaHA could be maintained at 1:30, since it was also their molar ratio in the film. The repeating unit of the NaHA polymer is the dimer formed by N-acetyl-D-glucosamine and D-glucuronic acid linked by a ß-1,3-glycosidic bond (dimer MW: 379.32 Da). A solution of cisPt at the same concentration without polymer was prepared and used as reference. Time-dependent changes in the absorbance of both cisPt solutions, with and without NaHA, were monitored on an UV-Vis spectrometer (V630, Jasco, Easton, MD, USA) in the wavelength range of 210 to 450 nm and at the following time points: 0, 1, 3, 8 and 24 h (T ≤25 °C). As mentioned earlier, the low molecular weight NaHA was used for this study since the solutions of cisPt with HMW NaHA could not be analyzed by UV spectroscopy because of their very high viscosity. It was expected that there would not be any difference in UV spectral changes irrespective of whether HMW or LMW NaHA are used because they are structurally similar except for the chain length.

Preparation of liquid film-forming mixtures and film manufacturing

For rheometry, DSC, FTIR-ATR and SEM-EDS analyses, film-forming mixtures (FFMs) were prepared with increasing concentration of cisPt, namely: 0 %, 0.066 %, 0.132 % or 0.264 % (w/w). The concentrations of HMW NaHA and other components in the mixture were as per the published composition (Ampollini et al., 2018; Banella et al., 2021). The composition of the four film-forming mixtures is given in Table 1, where the PVA helped in the film formation owing to its excellent film-forming properties (Ghezzi et al., 2023). Indeed, the films were too brittle and difficult to handle in its absence. The other components in the formulation (sorbitol 70% w/v, PEG 1000 stearate, and PEG 200) served as plasticizers. The FFMs were prepared by first dissolving the plasticizers in water, and then PVA was added and dissolved at 75 °C in two hours. Finally, cisPt and sodium hyaluronate were added. HMW NaHA was the last component added because its hydration took 18 h under mechanical stirring, and at the end the mixture became very viscous.

Table 1
Composition of the film-forming mixture (FFM) by weight/volume (% w/v). The four FFMs differed for the cisPt concentration only.

Component	% (w/v)
Sodium hyaluronate (HMW NaHA)	2.5
PVA 83,400 Da (87 % hydrolysis degree)	1
PEG 200	1
PEG 1000 stearate	1
Sorbitol 70 % (w/v)	1
Cisplatin (cisPt)	0, 0.066, 0.132, 0.264
Water	q.s. 100

The dry films were obtained by layering viscous FFMs on glass plates by means of a variable opening casting knife (BYK Gardner, gap 2 mm; BYK, Geretsried, Germany) (Riccio et al., 2022). The knife was set to have a 2 mm-thick layer. The wet layers were oven-dried at 55 °C for 8 h.

Determination of rheological properties of the film-forming mixtures containing increasing cisplatin concentration

The rheology of the four FFMs listed in Table 1 was determined using a high-resolution oscillatory rheometer (Mod. Stresstech HR; REOLOGICA Instruments AB, Skane, Sweden). The experiments were carried out using a stainless-steel plate-plate geometry (25 mm diameter; 1.0 mm gap). The temperature was set at 25 °C during experiments (Peltier T control). The shear viscosity and shear G' and G'' moduli were measured during oscillation regimen at a frequency of 1 s^{-1} by using a strain sweep shear test ranging from 0.1 to 4.5 %. Under these settings, the linear viscosity for the FFM containing 2.5 % (w/v) HMW NaHA without cisPt, was determined. Then, the viscoelasticity of the other three FFMs was measured under the same experimental settings at the following cisPt concentrations: 0.066 %, 0.132 % and 0.264 % (w/v). Shear viscosity (η) and G' and G'' moduli were measured in the frequency range from 0.01 to 10 s^{-1}. Frequency sweeps were performed at a controlled constant strain amplitude of 0.6 % to carry out the test within the linear viscoelastic region. All experiments were performed in triplicate.

Differential scanning calorimetry (DSC) of film-forming mixtures and films

For the DSC analysis of FFMs containing at 0 %, 0.033 % and 0.264 % cisPt (Table 1), samples (5 to 10 mg each) were placed into aluminum pans at room temperature. Afterwards, the pans were sealed and four pinholes were made. Scans were conducted with a DSC Q200 thermal analyzer (TA Instruments, New Castle, DE, USA). Samples were cooled down to −80 °C (10 °C/min), equilibrated for 5 minand then heated up to 250 °C at a heating rate of 10 °C/min under a dry nitrogen gas purge (50 cc/min).

DSC analyses of films were carried out on the drug-free placebo film and a 1 % (w/w) cisPt-loaded film. Accurately weighed pieces of the films (10.0 ± 0.5 mg each) were placed into aluminum pans at room temperature. Pans were sealed and four pinholes were made on the lids so that any vapor generated upon heating could escape. Samples were heated up to 250 °C at a heating rate of 10 °C/min under a dry nitrogen gas purge (50 cc/min). Differently from the analysis of the FFMs, no cooling scans were carried out. All data were analyzed by TA Universal Analysis 2000 software.

FTIR-ATR analysis of films

FTIR-ATR spectra of cisPt raw material (powder) and films with and without drug were acquired with a resolution of 2 cm^{-1} by using an Agilent Cary 660 spectrometer (Agilent Technologies, Santa Clara, CA, USA) that was equipped with extended beam splitter, DTGS detector, Pike ATR diamond cell, and a zinc selenide (ZnSe) crystal at 45°. The sample compartment of the equipment was continuously purged with Balston FT 80 drying system to eliminate carbon dioxide and water vapor.

Film morphology by scanning electron microscopy (SEM)

The surface analysis of films was performed on a Cambridge StereoScan 660 microscope (KEYENCE ITALIA S.p.A., Milan, Italy). The pressure variable mode was applied to Scanning Electron Microscope (SEM) to collect the images of film surfaces. An Energy Dispersive Spectroscopy (EDS) equipment was fitted with the SEM to determine the chemical composition of the film surface.

Results and discussion

HMW NaHA polymer lost weight from 0 to 600 °C with residual ashes

The thermal properties of HMW NaHA raw material (powder) used for the preparation of cisPt-hyaluronan films were analyzed by thermogravimetric analysis (TGA), and the results are shown in Fig. 2.

The initial weight loss (−9.9 %) between 40 and 120 °C was assigned to moisture evaporation (Loss I in Fig. 2). Then, between 200° and 520 °C thermal breakdown of NaHA occurred. In detail, a sharp weight loss zone was detected between 200 and 260 °C (Loss II), then relatively slow decompositions took place in the range 260–400 °C (Loss III), and also between 400 and 700 °C (Loss IV), which indicated the complete breakdown of polysaccharide residue. Overall, NaHA showed about 89 % weight loss by TGA. These thermogravimetric data for NaHA are in agreement with the literature (Sheu et al., 2016). They were used to determine the% by weight of NaHA for the subsequent determination of dn/dc in size exclusion chromatography with triple detection.

NaHA molecular weight distribution was unimodal with a weight average molecular weight (Mw) of 1080 kDa

One of the ways the physicochemical properties of the HMW NaHA used in the present investigation for film manufacturing were studied, was by measuring its weight average molecular weight (Mw). The Mw was determined by size exclusion chromatography (SEC), which separates macromolecules in solution according to their sizes. The SEC apparatus was equipped with a triple detector (TD), where (i) the laser diffractometer provided a direct measurement of molecular weight, (ii) the refractive index (RI) detector assessed the RI increment (dn/dc), and (iii) the viscometer was used to determine the gyration radius, *i.e.*, the size of the molecular coil. Fig. 3 shows the curve obtained from the SEC-TD analysis of the HMW sodium hyaluronate.

The SEC analysis required the use of 0.1 M $NaNO_3$ as the mobile phase to have sufficient ionic strength to disrupt any aggregate formed by the interaction between the polar polymer chains in solution (Teresa et al., 2001). At lower ionic strength, the elution of the aggregated structures would increase the hydrodynamic volume and retention time, leading to an overestimation of the polymer molecular weight. There was no need to use more concentrated $NaNO_3$ than 0.1 M as no aggregates were detected upon elution (data not shown). In these conditions, number average molecular weight (Mn) and weight average molecular weight (Mw) were determined and are reported in Table 2. Mn is associated with the molar concentration, whereas Mw is associated with the mass concentration. If all polymer chains were of equal length, Mn would be equal to Mw and the polymer would be monodisperse. The polymer polydispersity is generally calculated by the Mw/Mn ratio that indicates the heterogeneity of the polymer chains. The higher the ratio, the broader the distribution of the molecular weights. NaHA had an Mw of 1080 kDa, which is in line with the information provided by the

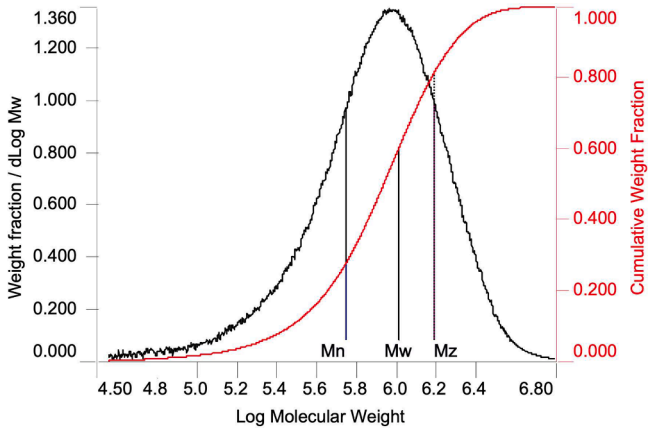

Fig. 3. SEC-TD curve of neat HMW NaHA (black) and cumulative weight fraction (red).

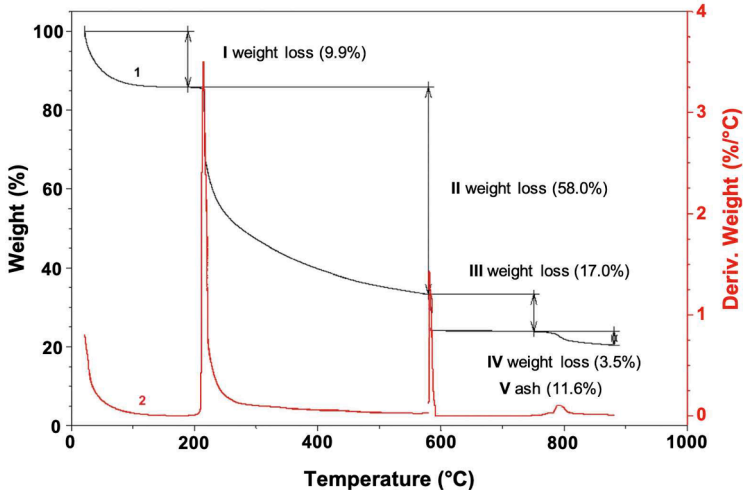

Fig. 2. TGA curves of neat NaHA (black; curve #1) and derivative weight (red; curve #2) under nitrogen flow till to 600 °C and then under oxygen up to 900 °C.

Table 2
The molecular weight values of HMW NaHA solutions (0.15 – 0.40 mg/ml) obtained by SEC-TD analysis (mean ± SD, $n = 3$).

Parameters	Value
[a]Mn (kDa)	698 ± 25
[b]Mw (kDa)	1080 ± 38
[c]Mz (kDa)	1579 ± 46.0
[d]Mp (kDa)	994 ± 27
[e]Mw/Mn	1.54
[f]IV (dl/g)	15.3 ± 0.9
[g]Rh (nm)	64.1
[h]Rg (nm)	94.0
[i]Mark-Houwink	0.496
[l]Mark-Houwink logK	−1.757
[m]Sample recovery (%)	99.2
[n]dn/dc (ml/g)	0.150

[a] Number average molecular weight.
[b] Weight average molecular weight.
[c] The third moment value of the polymer distribution.
[d] The most probable molecular weight (peak value).
[e] Polydispersity (Mw/Mn).
[f] Intrinsic viscosity.
[g] Hydrodynamic radius.
[h] Gyration radius.
[i] Slope of Mark-Houwink equation.
[l] Intercept of Mark-Houwink equation.
[m] The percentage of the sample analyzed determined by dn/dc value.
[n] Refractive index to concentration ratio determined by analysis of the different concentration of HMW NaHA solutions ranging from 0.15 to 0.40 mg/ml in the same experimental conditions.

manufacturer.

Table 2 reports all the relevant parameters calculated by the Omnisec v4.6 dedicated software (Malvern Panalytical, Malvern, London, UK) for triple detection SEC-TD analysis.

The sample recovery during SEC was equal to 99.2 %, indicating the HMW NaHA used was very pure. The last parameter obtained was the dn/dc ratio, which can be used to determine the exact concentration of NaHA in a sample of unknown concentration. The value of dn/dc is unique for each combination of polymer and solvent at a given wavelength and temperature, since it represents the difference in the RI between the sample and the solvent.

Subsequently, it was planned to use SEC-TD on the HMW NaHA solution after the addition of cisPt, to assess whether it would change NaHA molecular weight. However, the addition of the drug made the solution too viscous for SEC analysis. Several attempts to decrease the viscosity by dilution with 0.1 M or higher $NaNO_3$ concentrations were unsuccessful. The conclusion was that cisPt interacted strongly with NaHA that could not be disrupted by $NaNO_3$.

cisPt coordination with NaHA was fast and UV spectroscopy could not visualize the intermediate step of cisplatin hydrolysis

Cisplatin is a square-planar coordination complex of platinum with two chloride ions, which are good leaving groups when cleaved by nucleophile species (Dasari & Tchounwou, 2014). After administration to the body, cisPt undergoes hydrolysis, *i.e.,* one chloride ion after the other is substituted by two water molecules respectively forming mono- and diaqua-complexes (aquaplatinum) (Makovec, 2019). The latter is the active species that cross-links DNA filaments. This ligand exchange (Cl^- leaves and H_2O enters) activates cisPt that should occur only in the cytoplasm of cancer cells. It can occur earlier though and cause unwanted interactions with other biomolecules in the bloodstream (Almeida & Dos Santos, 2023). The cisPt hydrolysis could also contribute to its complexation with NaHA. In this regard, Zhang et al. (2011) applied UV-Vis spectroscopy to study the complexation between cisPt and chondroitin sulfate, whose structure is very similar to NaHA. In the present investigation, using a water solution of cisPt, we collected its UV spectra over a 24 h period, during which the aqua complexes would certainly be formed (Hindmarsh, 1998). The aqua complexes could be distinguished from cisPt based on their different maximum wavelength (λ_{max}) of absorbance (Fig. 4A). In fact, the UV spectrum of the cisPt solution at time 0 showed a peak at 300 nm. The peak was broad and poorly symmetric with a small shoulder at 270 nm. As time passed, the absorbance intensity decreased at 300 nm and increased at 270 nm. Eventually, at 24 h, there was a neat peak at 270 nm, which was attributed to the hydrolyzed products (aquaplatinum), as suggested by Zhang et al. (2011). No further changes of cisPt spectrum were observed beyond 24 h, suggesting that the hydrolysis of cisPt reached an equilibrium in 1 day at 25 °C.

As shown in Fig. 4B, the addition of NaHA totally modified the spectral behavior compared to cisPt alone (time 0). As mentioned earlier, a low molecular weight NaHA was used to control the solution viscosity. NaHA is a polysaccharide and does not absorb UV radiation above 210 nm. No absorbance peak was observed at 300 nm nor at 270 nm to detect cisPt or aquaplatinum. Instead, a steep and continuous increase of absorbance from 300 nm toward lower wavelengths was noticed with an inflection point between 244 and 256 nm. These spectral changes indicated the possibility of the formation of a new product, probably the cisPt/NaHA complex. We could not verify whether the inflection point corresponded or not to the presence of intermediate aquaplatinum during the complex formation. Nevertheless, as time passed and more complex formed, the inflection point progressively smoothed out till it disappeared completely at 24 h.

Taken together, the changes in UV spectra signify the cisPt/NaHA complex formation. The intermediate formation of the aqua complexes of Pt^{2+} was not unequivocally ascertained, differently from the observations of Zhang et al. (2011) in their work with chondroitin sulphate. One reason could be that the interaction of cisPt with NaHA was faster than that with chondroitin sulphate; as some cisPt/NaHA complex formed early, its absorbance became predominant. Contrarily, the slower complexation between cisPt and chondroitin sulphate had given the time for the UV spectrum of cisPt to change first to that of aquaplatinum and then, after 24 h, to the spectrum of the new species formed. The complexation between cisPt and NaHA reached the equilibrium in 24 h. When the UV spectra of the cisPt/NaHA complex were acquired again at 32 and 48 h, they perfectly overlapped with the one at 24 h (data not shown).

cisPt coordination by hyaluronan increased the viscosity and modified the viscoelasticity of the film-forming mixture due to cross-linking

Polymer solutions flow more easily under the effect of increasing shear rate. The viscosity of a polymer fluid is its resistance to flow or creep. When the shear rate is directly proportional to the shear stress, the fluid has Newtonian behavior, and the viscosity is constant. Non-Newtonian fluids show a nonlinear relationship between shear rate and shear stress, thus their viscosity changes. As is known, the polymer solutions of NaHA in water behave as non-Newtonian systems. They show shear thinning behavior, *i.e.*, their viscosity decreases at increasing shear stresses (Bother & Waaler, 1990). This behavior is explained by the fact that these high molecular weight polymers reflect the interpenetration or entanglement of the polymer chains, resulting in solvent immobilization. Under the action of a shear rate, the entangled macromolecules tend to align along the direction of flow. The result is a decrease in fluid viscosity.

The rheology of fluid systems containing cisPt and NaHA has never been reported in the literature. Some authors reported that salts containing ions of Hofmeister series influenced the viscosity of hyaluronan solutions (Musilová et al., 2019). Without emphasizing the chemical groups actually involved in cisPt/NaHA coordination, we may expect that the complexation could change the rheology of the film-forming

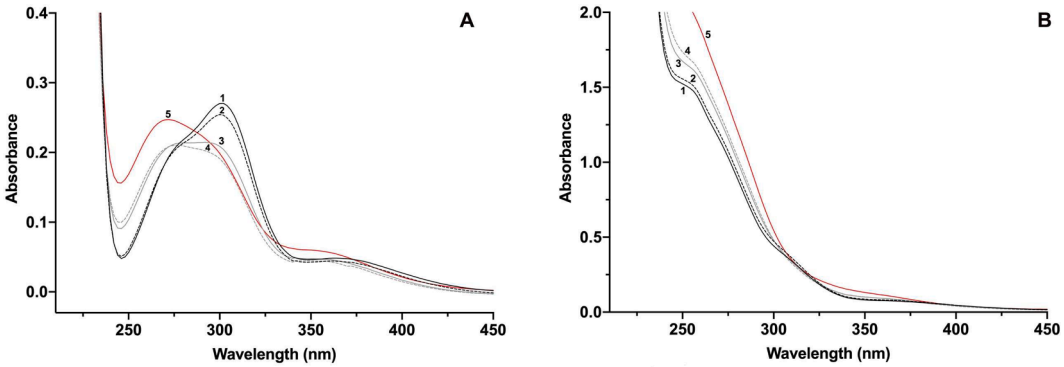

Fig. 4. UV spectra of cisPt solutions in water: (A) 0.066 % (w/v) cisPt alone and (B) 0.066 % (w/v) cisPt with 2.5 % (w/v) LMW NaHA. The NaHA polymer was of molecular weight of 76 kDa, *i.e.*, ~1/10 that of the HMW NaHA used for film manufacturing. For both solutions, the spectra were acquired at 0 h (solid black; spectrum #1), 1 h (dashed black; spectrum #2), 5 h (solid grey; spectrum #3), 8 h (dashed grey; spectrum #4) and 24 h (red; spectrum #5).

mixture (FFM). Thus, we measured the viscosity of four FFMs at the same NaHA concentration (2.5% w/v). Conversely, cisPt concentration was varied in the range 0–0.264 % (w/v). These concentrations corresponded to 0, 1, 2 and 4 % (w/w) cisPt in the film on dry basis. All mixtures, except the drug-free one, should contain the cisPt/NaHA complex. The dependence of viscosity on shear rate of the four samples is shown in Figs. 5(A–D).

The rheograms show that the zero-shear viscosity (η_0, *i.e.*, the viscosity at the lowest tested shear rate, which was 0.01 s^{-1}) strongly depended on the concentration of cisPt in all tested samples. The rheological data are summarized in Table 3.

Interestingly, the zero-shear rate viscosity (η_0) could vary from 105 to 994 Pa•s as a function of cisPt concentration due to its coordination with NaHA. The mixtures exhibited the expected non-Newtonian shear thinning behavior, since NaHA macromolecules are highly entangled. The entanglements decreased the shear flow at low shear rates. Conversely, at high shear rates, NaHA macromolecules could be disentangled and aligned towards the shear field. The largest shear thinning

Table 3
Rheological properties of the film-forming mixtures containing increasing cisPt concentrations. Values are the mean ± SD ($n = 3$).

cisPt	[a]zero-shear viscosity	[b]Shear complex viscosity at 1 s^{-1}	[c]Shear moduli at 1 s^{-1}	
(% w/v)	Pa•s	Pa•s	G' (Pa)	G'' (Pa)
0.0	105.1 ± 4.1	37.1 ± 2.4	191.2 ± 9.0	130.2 ± 6.5
0.066	320.5 ± 9.5	66.5 ± 4.1	384.3 ± 11.7	149.4 ± 5.7
0.132	415.5 ± 11.5	78.6 ± 4.6	479.4 ± 13.9	153.4 ± 4.9
0.264	993.6 ± 22.3	192.1 ± 9.7	1152.2 ± 17.7	419.5 ± 12.2

[a] zero-shear viscosity (η_0) was measured at 0.01 s^{-1}.
[b] shear viscosity at 1 s^{-1}.
[c] storage modulus G' and loss modulus G'' at 1 s^{-1}.

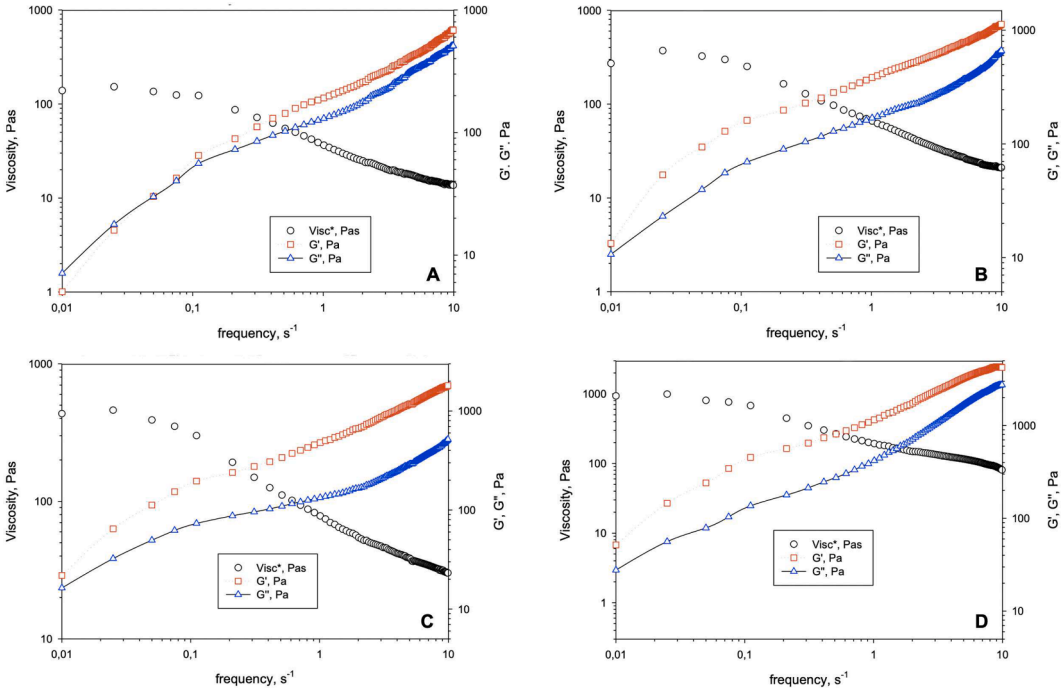

Fig. 5. Rheological behavior of film-forming mixtures (HMW NaHA 2.5% w/v) at increasing cisPt concentration (% w/v): (A) 0 %, (B) 0.066 %, (C) 0.132 %, and (D) 0.264 %. The black trace is the viscosity (η, Pa•s), while red and blue traces are the storage (G') and loss (G'') moduli, respectively. Shear rate frequency ranged between 0.01 to 10 s^{-1}.

behavior was observed at the cisPt concentration of 0.264 % (w/v). If complexes are formed with NaHA, the molecular weight of the polymer increases due to a larger number of such entanglements. Consequently, η_0 was higher and the shear thinning behavior stronger (Rebenda et al., 2020). In contrast, the shear thinning at low cisPt concentration, *i.e.*, with less cross-links, was relatively weak and occurred across a very narrow range of shear rates (oscillation frequency). The least concentrated sample exhibited almost Newtonian behavior.

Besides viscosity, hyaluronic acid solutions/gels also show elastic properties. When they are deformed under the effect of a shear stress, they tend to store elastic strain energy to a certain degree and bounce back to their original shape when the deforming stress is removed. Elastic deformation and polymer viscous flow combine as viscoelasticity. Oscillation rheology allows characterization of the viscoelastic properties of a polymer solution by imposing small-amplitude oscillatory shear to the sample and observing the response. By using storage (G') and loss (G") moduli, the relative amounts of energy stored elastically (G') and dissipated viscously (G'') through deformations are typically plotted as a function of deformation frequency to obtain a viscoelastic fingerprint of the material.

Values of G' and G" of all tested film-forming mixtures at 1 s^{-1} frequency are reported in Table 3. Figs. 5(A-D) show that the storage (G') and loss (G'') moduli were dependent on the frequency of oscillating motion as expected for a non-Newtonian system. The viscoelastic properties exhibited predominantly elastic-like behavior across the whole range of tested frequencies, since the G' values were always higher than the G'' values. Only the NaHA solution without cisPt (*i.e.*, without the complex) exhibited a viscoelastic behavior characterized by a crossover point at 0.05 s^{-1} (Fig. 5A). Before this point, G'' was higher than G', while G' became higher than G'' after this point. The crossover point indicates the oscillation frequency at which a transition occurs from viscous to elastic behavior. Normally, the system shows viscous behavior at low frequencies because the molecular chains can release the stress received by chain disentanglement and molecular rearrangement during the period of oscillation. In contrast, at high oscillation frequencies, chains do not have enough time to disentangle because of the short period of oscillating motion, and, therefore, the system exhibits elastic behavior (Rebenda et al., 2020). The FFM without cisPt behaved according to this scheme and showed the crossover point. In contrast, in the whole frequency range considered (0.01 –10 s^{-1}), there was no crossover point for the cisPt-containing FFMs. The storage modulus (G') of film-forming mixtures at any cisPt concentration was above the loss modulus (G'') at all frequencies. It means that the system was always more elastic than viscous by storing, and not dissipating, the energy produced by the oscillatory motion. This confirms the presence in these systems of a network of polymer chains cross-linked by platinum. The coordination bonds made the chains unable to release the stress by disentangling at none of the frequencies considered (Muljana et al., 2022). The available rheometer did not work at frequencies lower 0.01 s^{-1}, thus we do not know whether a crossover point existed before 0.01 s^{-1}. As the magnitude of G' modulus increased with the content of cisPt/NaHA complex, the crossover point could have shifted to lower frequencies. The crossover point frequency is important also because it determines the extent by which the fluid absorbs or dissipates energy (Rebenda et al., 2020). The reciprocal of the crossover point is the relaxation time, *i.e.*, the time required for a viscous substance to recover from shearing stress after the flow has ceased. In summary, the absence of G'/G'' moduli crossover point in the liquid film-forming mixtures with cisPt can be interpreted in terms of the formation of a cisPt-mediated non-reversible cross-linking network within the polymer structure. The cross-linking was "non-reversible" since cisPt is not displaced from NaHA.

The cisPt/NaHA complex in the film-forming mixture and film caused water to evaporate at lower temperature in DSC

DSC analyses (cooling and heating scans) of film-forming mixtures were carried out to determine whether there were any differences in the system's thermal behavior as a function of cisPt presence and concentration. We selected the two extremes (0.033 % and 0.264% w/v) of the concentration range considered in the rheological studies. All the other components in the mixture, including HMW NaHA, were at the concentrations reported in Table 1. DSC scans in Fig. 6 show the melting of solid water at 2 °C and its subsequent evaporation. The temperature values of the evaporation events are displayed.

In the FFM without cisplatin, the polymer was fully hydrated with water molecules bound to hydroxyl and carboxylate groups of NaHA via hydrogen bonds. This exhibited an endothermic peak of water evaporation at 106.75 °C. In contrast, the FFMs containing cisPt, in particular at its highest concentration, showed the onset of evaporation at a lower temperature. The endotherm peak was at 101.77 °C for the FFM at 0.264 % cisPt. The evaporation of water, at least some of it, appeared to be easier, which could be connected to the formation of the cisPt/NaHA complex. Indeed, if evaporation required less heat, it meant that water molecules were freer to escape. Pt^{2+} coordination would "occupy" functional groups of the polymer formerly involved in the interaction with some H_2O molecules and displace them. Consequently, these molecules could require less heat to evaporate. According to this interpretation, the FFM at lower cisPt concentration had less water molecules displaced by Pt^{2+} and little effect on the evaporation temperature of water.

The differences in the evaporation temperature of water from the FFMs attributed to the complex formation were small. This could be due to the fact that the FFM contained only about 7 % (w/v) of total solids dissolved, including cisPt, while the rest of the composition was water. Only a small part of this water would have been affected by the interaction between cisPt and NaHA. Thus, it was more appropriate to study the effect of cisPt/NaHA complexation on the thermal properties of films with much less moisture content. The resulting thermograms on the 1 % (w/w) film (composition of its FFM at 0.066% cisPt according to Table 1) are reported in Fig. 7.

In both DSC scans of the drug-free film *vs.* the 1% (w/w) cisPt-loaded one in Fig. 7, the first event was water evaporation (endotherm), which was then followed by the melting of semicrystalline PVA around 200 °C (endotherm). The PVA endotherm was immediately followed by a thermal event that appeared to be an exotherm, which could be due to NaHA decomposition. This exothermic event, however, occurred at around 210 °C, *i.e.*, at a lower temperature than that for the HMW NaHA raw material (230 °C; Fig. S1 in Supplementary Material). The thermal behavior of the films differed in that the water evaporation temperatures were 96 °C and 80 °C, respectively for the drug-free and drug-loaded films, confirming that the presence of cisPt eased water evaporation, as observed for the film-forming mixtures (Fig. 6). Since both the placebo and the cisPt-loaded films had the same low residual moisture content (10% w/w), a reasonable interpretation for the difference in their water evaporation endotherms could be the one given for the FFMs; the binding of cisPt to NaHA (complex formation) involved binding sites on the polymer macromolecules previously occupied by water molecules, making the water free to evaporate with less heat.

Although there is a potential that NaHA could also interact with PVA present in the film, as observed by Pan et al. (2020), no definitive mechanism for any interaction between the two polymers could be elucidated by the thermal studies here reported, since the endothermic-exothermic events observed at high temperature were rather complex due to concurrent melting and degradation. Since both NaHA and PVA are water-soluble polymers with numerous -OH groups in their structures, the miscibility between them could be due to hydrogen bonding.

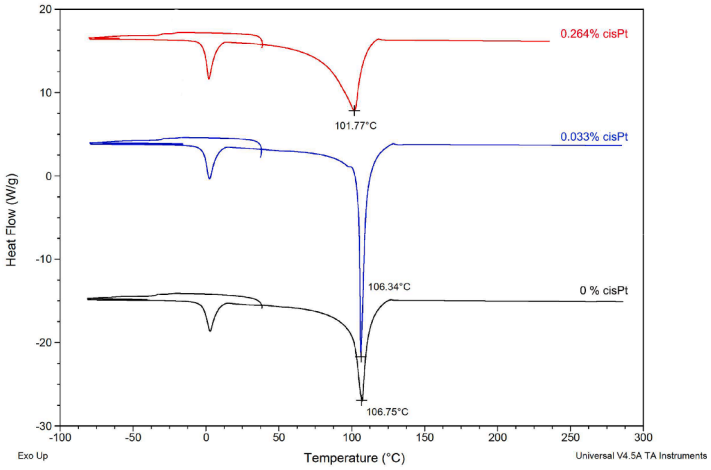

Fig. 6. DSC scans of the film-forming mixtures at increasing cisplatin concentration (% w/v): 0 % (black), 0.033 % (blue), and 0.264 % (red).

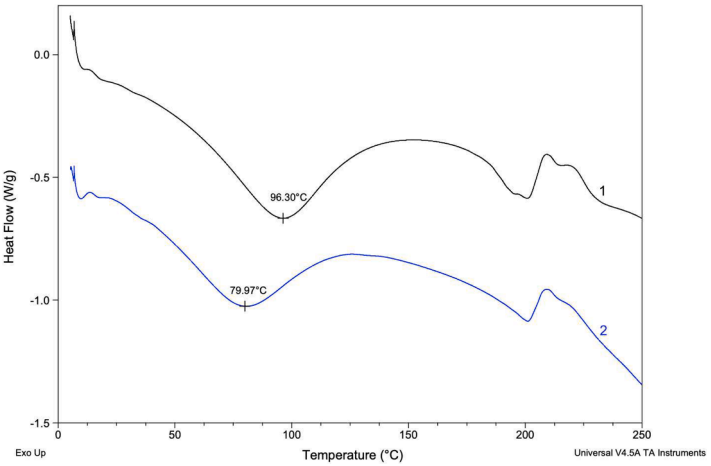

Fig. 7. DSC scans of drug-free film (black; scan #1) and 1% (w/w) cisPt-loaded film (blue; scan #2).

FTIR-ATR spectra indicated that cisPt/NaHA complex formation may involve the carboxylate group

Fig. 8 shows the spectra of films loaded with cisPt at different concentrations together with the spectra of neat cisPt and of the placebo film without drug.

The vibrational bands at 3280 and 3199 cm^{-1} in the spectrum of cisPt powder (raw material), assigned to symmetric and asymmetric N—H stretching, were not observed in the films, neither with nor without drug. In fact, N—H stretching bands were completely hidden by the O—H stretching of the NaHA polymer. The O—H stretching band was broad, indicating that -OH groups were involved in intermolecular

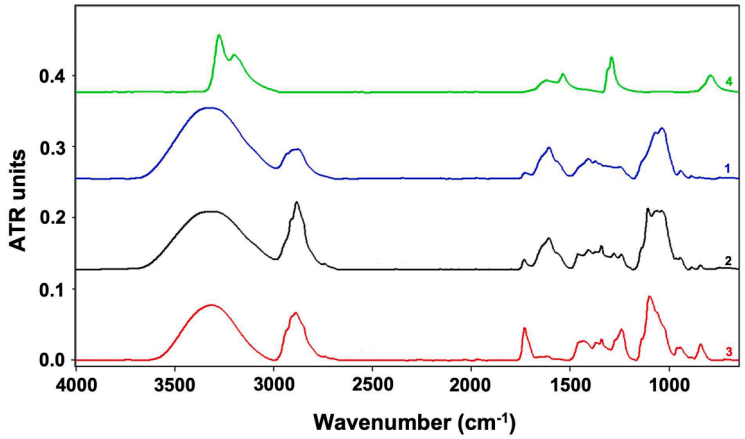

Fig. 8. FTIR-ATR spectra of films containing different cisPt concentrations: 0% w/w (placebo film; blue, spectrum #1), 1% w/w (black, spectrum #2), 4% w/w (red, spectrum #3). The spectrum of cisPt powder (raw material; green, spectrum #4) in the same wavenumber range is reported for comparison purposes.

hydrogen bonds. The other bands of neat cisPt at 1625 cm^{-1} and, more prominent, 1413 cm^{-1} were assigned to H—N—H bending (Yang et al., 2020). The remaining vibrational bands of cisPt at 1378 and at 800 cm^{-1} were attributed to H—N—H deformations out of plane and in the plane (rocking), respectively. The N—H vibrational bands of the amide group were not observed in the placebo NaHA film, likely because they were present in the same region where asymmetric C═O (1610 cm^{-1}) and symmetric C—O (1410 cm^{-1}) stretching modes of carboxylic groups occur (Gilli et al., 1994).

Then, comparing the spectra of cisPt-loaded films and the placebo film, changes were noticed due to cisPt presence in the films as a function of its concentration. Indeed, while the film loaded with low cisPt concentration (1% w/w) had a quite similar spectrum to placebo, the spectrum of the more concentrated film (4% w/w) showed some differences in the spectral range between 1500 and 1100 cm^{-1}. Several bands appeared in this range attributed to bending and deformation of the carbohydrate ring. The strongest band around 1100 cm^{-1} was reasonably attributed to ether -C—O- stretching in the NaHA polymer chain (Yang et al., 2020). The presence of cisPt at the higher concentration caused the shift of C═O stretching from 1610 to 1730 cm^{-1} as well as the shift of C—O stretching from 1410 to 1235 cm^{-1}. Gilli et al. (1994) reported similar shifts in the spectrum of hyaluronan polymer alone when changing from deprotonated to protonated form. More recently, a definitely smaller shift of the carboxylate signal from 1630 to 1635 cm^{-1} was considered a proof of the interaction between cisplatin and eumelanin nanoparticles (Atik et al., 2023). If $-COO^-$ was the group involved in the interaction with cisPt, similar changes of its stretching bands would occur. Actually, an analogous shift was not observed for the film at lower cisPt concentration, where less interactions between cisPt and NaHA would lead to poor signal. Interestingly, the cisPt band at 800 cm^{-1}, attributed to the plane deformation of H—N—H, disappeared in the drug-loaded films, although the carbohydrate polymer has no strong vibrational bands in this wavenumber range that may hide it. This observation suggests an important distortion of the H—N—H bonds of cisplatin, occurring as cisPt and NaHA formed the complex in the film. Furthermore, it should be considered that strong hydrogen bond interactions can establish between -NH of cisPt and -OH of the carbohydrate, contributing to interchain interactions. Together with the coordination mediated by Pt^{2+}, these interactions are in agreement with the shear viscosity increase as a function of cisPt concentration observed for the film-forming mixtures. However, in carbohydrate polymers, strong interchain interactions are generally also observed between polar groups of the polymer itself, mainly due to the high molecular weight. Thus, the existence of polar compounds such as cisPt/NaHA complex can only increase this effect.

EDS coupled to SEM microscopy evidenced that the cisPt/NaHA complex in films had the form of a network of aggregates

The morphology of the surface of the two cisPt-loaded films analyzed by FTIR-ATR was then investigated by Scanning Electron Microscopy (SEM) in combination with an Energy Dispersive Spectroscopy (EDS) probe to obtain the microchemical analysis of the observed surface areas. EDS is an analytical technique, usually combined with SEM, that enables the chemical characterization and analysis of materials. The sample excited by an energy source (such as the electron beam of the microscope) dissipates some of the absorbed energy by ejecting core-shell electrons. The higher energy outer-shell electrons then proceed to fill their places, releasing the difference in energy as an X-ray that has a characteristic spectrum based on its atom of origin. This allows for the compositional analysis of a given sample that has been excited by the energy source. The position of the peaks in the spectrum identifies the element, whereas the intensity of the signal corresponds to the concentration of the element.

Fig. 9A shows the SEM image of the film with the lower content of cisPt. EDS identified the chemical composition of individual zones across the film surface observed (zone #19 and #22 in Fig. 9A). The white aggregates (spectrum #22) contained platinum, thus corresponded to the cisPt complex present within the NaHA polymer matrix (Table 4). On the other hand, the grey zone in Fig. 9A (spectrum #19) represented the NaHA polymer matrix, because EDS analysis did not detect Pt atoms in that zone of the film surface (Table 4).

The image of Fig. 9B shows that when cisPt was loaded in the film at 4-times higher concentration, more aggregates with irregular shapes and variable sizes were observed. The EDS spectrum confirmed that there was platinum in the aggregates (Table 4), likely coordinated to hyaluronan. The amount of platinum detected (7 % by weight) was exactly four times the amount quantified by EDS in the low concentration film (1.7 % by weight), which is in agreement with the theoretical cisPt concentration. The observed aggregates suggest that the cisPt/NaHA complex within the carbohydrate polymer matrix gave rise to a quite entangled network visible on the film surface. The existence of a

Table 4
Chemical composition by EDS spectra of individual zones across the surface of films as a function of cisPt concentration (N.D.: not detected). The spectrum's zones of interest are numbered in the images.

Element	1 % cisPt film		4 % cisPt film	
	Spectrum 22 (% w/w)	Spectrum 19 (% w/w)	Spectrum 14 (% w/w)	Spectrum 17 (% w/w)
C	69.7 ± 0.2	67.1 ± 0.2	61.5 ± 0.2	64.8 ± 0.2
O	27.6 ± 0.2	32.3 ± 0.2	29.3 ± 0.2	32.0 ± 0.2
Pt	1.7 ± 0.1	N.D.	7.0 ± 0.1	N.D.
Cl	0.5 ± 0.0	N.D.	1.0 ± 0.0	0.3 ± 0.0
Na	0.5 ± 0.0	0.6 ± 0.0	1.2 ± 0.0	2.9 ± 0.0

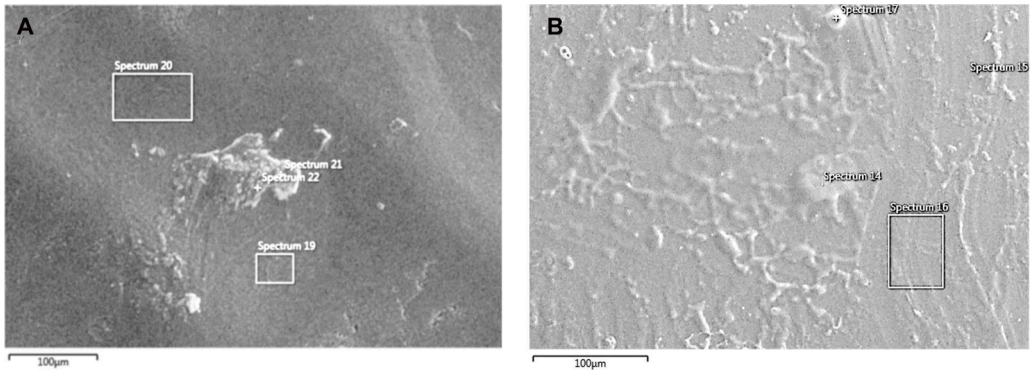

Fig. 9. SEM images of the surface of the NaHA films containing: (A) 1 % (w/w) cisPt and (B) 4 % (w/w) cisPt.

network agrees with the results of rheological measurements and FTIR-ATR vibrational spectroscopy.

Conclusions

It was previously demonstrated that the cisplatin/hyaluronan complex formed between the anticancer drug and the carbohydrate polymer in the film designed for loco-regional treatment of pleural mesothelioma had higher activity and low toxicity *in vivo* as compared to cisPt alone (Ampollini et al., 2010, 2018; Banella et al., 2021). The present investigation has provided further insight into the nature of the complexation between the two components. By SEC analysis with triple detector, the molecular weight of the carbohydrate polymer (NaHA) used for manufacturing the film, was confirmed to be ~1 million Da, and the material was highly monodispersed. A direct proof of the rapid interaction between cisPt and NaHA was given as the UV spectroscopic behavior of a cisPt solution in water changed following the addition of NaHA. Differential scanning calorimetry suggested that the complex formation occurred via an exchange of ligands on functional groups of the NaHA macromolecule that normally bound water molecules without cisPt around. The effect of the interaction was such that the rheology of the film-forming mixture made with the high molecular weight hyaluronan polymer, was completely modified by the presence of cisPt. This result must have an important role in the loco-regional drug release on the pleural mesothelium. The system turned from its typical viscoelasticity without cisPt to a "solid-like" behavior caused by the entangling action of platinum. The stiffness of the material depended on cisPt concentration. So far, at the cisplatin concentrations adopted for the films studied *in vivo* (0.5 % and 1% w/w), the viscosity of the corresponding film-forming mixtures (FFM) has not hampered the manufacturing of the films. However, the effect of higher drug concentrations on the FFM viscosity must be known in anticipation of the need to increase the dosage.

Based on FTIR-ATR spectroscopy data on films, the interaction between drug and polymer appeared to be mediated by the carboxylate groups substituting the chloride ions in Pt^{2+} coordination. This coordination left Na^{+} and Cl^{-} ions as "spectator elements", which were present in equal amount on the film surface zones where platinum was detected by SEM-EDS. The film surface showed a network of aggregates whose number, shape and size were dependent on cisPt concentration. Such a three-dimensional network was built by the formation of complex, which also provides the evidence of strong interchain interactions involving H—N—H groups. However, the aggregates depicted a non-homogeneous film composition. We know from previous quantitative analyses (Banella et al., 2021) that the FFM is homogeneous with respect to cisPt concentration. This observed surface structure and apparently inhomogeneous composition of the dry film may have resulted from intermolecular rearrangements occurred during the drying process.

Funding statement

This research did not receive any specific grant from funding agencies in the public, commercial, or not-for-profit sectors.

CRediT authorship contribution statement

Sabrina Banella: Writing – review & editing, Writing – original draft, Methodology, Investigation, Formal analysis, Data curation, Conceptualization. **Abu T.M. Serajuddin:** Writing – review & editing, Supervision, Resources, Methodology. **Gaia Colombo:** Writing – review & editing, Supervision, Resources, Project administration, Methodology, Data curation, Conceptualization. **Marco Scoponi:** Writing – original draft, Validation, Resources, Methodology, Investigation, Formal analysis, Data curation.

Declaration of competing interest

The authors declare that they have no known competing financial interests or personal relationships that could have appeared to influence the work reported in this paper.

Acknowledgments

The Authors owe heartfelt gratitude to Dr. Fabrizio Bortolotti, prof. Paolo Colombo and Dr. Paolo Marchetti for the technical support and fruitful scientific discussions.

Supplementary materials

Supplementary material associated with this article can be found, in the online version, at doi:10.1016/j.carpta.2024.100436.

References

Almeida, E. R., & Dos Santos, H. F. (2023). Nanoconfinement effect on the hydrolysis of cisplatin. *Chemical Physics Letters, 811*, Article 140247.
Amano, Y., Sakura, K. L., Ohta, S., & Ito, T. (2022). Cisplatin-chelated iminodiacetic acid-conjugated hyaluronic acid nanogels for the treatment of malignant pleural mesothelioma in mice. *Molecular Pharmaceutics, 19*, 853–861.
Ampollini, L., Barocelli, E., Cavazzoni, A., Petronini, P., Mucchino, C., Cantoni, A. M., et al. (2018). Polymeric films loaded with cisplatin for malignant pleural mesothelioma: A pharmacokinetic study in an ovine model. *Journal of Thoracic Disease, 10*, S207–S220.
Ampollini, L., Sonvico, F., Barocelli, E., Cavazzoni, A., Bilancia, R., Mucchino, C., et al. (2010). Intrapleural polymeric films containing cisplatin for malignant pleural mesothelioma in a rat tumor model: A preliminary study. *European Journal of Cardio-Thoracic Surgery, 37*, 557–565.
Atik, A., Günal, T., Bozkurt, P. A., Köse, S. N., Alp, B., Yandım, C., et al. (2023). Characterization of cisplatin loaded hydrophilic glycol chitosan modified eumelanin nanoparticles for potential controlled-release application. *Journal of Drug Delivery Science and Technology, 84*, Article 104440.
Banella, S., Quarta, E., Colombo, P., Sonvico, F., Pagnoni, A., Bortolotti, F., et al. (2021). Orphan designation and cisplatin/hyaluronan complex in an intracavitary film for malignant mesothelioma. *Pharmaceutics, 13*, 362.
Banella, S., Saraswat, A., Patel, A., Serajuddin, A. T. M., Colombo, P., Patel, K., et al. (2023). *In Vitro* assessment of cisplatin/hyaluronan complex for loco-regional chemotherapy. *International Journal of Molecular Sciences, 24*, 15725.
Bother, H., & Waaler, T. (1990). Rheological characterization of tear substitutes. *Drug Development and Industrial Pharmacy, 16*, 755–768.
Boztepe, T., Castro, G. R., & León, I. E. (2021). Lipid, polymeric, inorganic-based drug delivery applications for platinum-based anticancer drugs. *International Journal of Pharmaceutics, 605*, Article 120788.
Cai, S., Xie, Y., Bagby, T. R., Cohen, M. S., & Forrest, M. L. (2008). Intralymphatic chemotherapy using a hyaluronan-cisplatin conjugate. *Journal of Surgical Research, 147*, 247–252.
Chai, Z., Teng, C., Yang, L., Ren, L., Yuan, Z., Xu, S., et al. (2020). Doxorubicin delivered by redox-responsive Hyaluronic Acid-Ibuprofen prodrug micelles for treatment of metastatic breast cancer. *Carbohydrate Polymers, 245*, Article 116527.
Cotton, F. A., Wilkinson, G., Murillo, C. A., & Bochmann, M. (1999). *Advanced inorganic chemistry* (6th ed.). New York: John Wiley and Sons.
Dasari, S., & Tchounwou, P. B. (2014). Cisplatin in cancer therapy: Molecular mechanisms of action. *European Journal of Pharmacology, 740*, 364–378.
Davoudi, M., Jadidi, Y., Moayedi, K., Farrokhi, V., & Afrisham, R. (2022). Ameliorative impacts of polymeric and metallic nanoparticles on cisplatin-induced nephrotoxicity: A 2011–2022 review. *Journal of Nanobiotechnology, 20*, 504.
Ghezzi, M., Ferraboschi, I., Fantini, A., Pescina, S., Padula, C., Santi, P., et al. (2023). Hyaluronic acid - PVA films for the simultaneous delivery of dexamethasone and levofloxacin to ocular tissues. *International Journal of Pharmaceutics, 638*, Article 122911.
Gilli, R., Kacuráková, M., Mathlouthi, M., Navarini, L., & Paoletti, S. (1994). FTIR studies of sodium hyaluronate and its oligomers in the amorphous solid phase and in aqueous solution. *Carbohydrate Research, 263*, 315–326.
Gold, J. M., & Raja, A. (2021). *Cisplatin*. Treasure IslandFL: StatPearls Publishing.
Hindmarsh, K. (1998). *Kinetic study of platinum complexes*. Ph.D. Thesis. Christchurch, New Zealand: University of Canterbury.
Ishiguro, S., Cai, S., Uppalapati, D., Turner, K., Zhang, T., Forrest, W. C., et al. (2016). Intratracheal administration of hyaluronan-cisplatin conjugate nanoparticles significantly attenuates lung cancer growth in mice. *Pharmaceutical Research, 33*, 2517–2529.
Kostova, I. (2006). Platinum complexes as anticancer agents. *Recent Patents on Anti-Cancer Drug Discovery, 1*, 1–22.
Makovec, T. (2019). Cisplatin and beyond: molecular mechanisms of action and drug resistance development in cancer chemotherapy. *Radiology and Oncology, 53*, 148–158.

Mirzaei, S., Khademi, Z., Zolfaghari, R., Ramezani, M., Alibolandi, M., Abnous, K., et al. (2023). Dual-targeted delivery system using hollow silica nanoparticles with H+-triggered bubble generating characteristic coated with hyaluronic acid and AS1411 for cancer therapy. *Drug Development and Industrial Pharmacy, 49*, 648–657.

Moura, M. J., Gil, M. H., & Figuereido, M. M. (2019). Cisplatin delivery systems based on different drug encapsulation techniques. *European Polymer Journal, 113*, 357–364.

Muljana, H., Remerie, K., Boven, G., Picchioni, F., & Bose, R. K. (2022). Cross-Linking of Polypropylene with Thiophene and Imidazole. *Polymers, 14*, 2198.

Musilová, L., Kašpárková, V., Mráček, A., Minařík, A., & Minařík, M. (2019). The behaviour of hyaluronan solutions in the presence of Hofmeister ions: A light scattering, viscometry and surface tension study. *Carbohydrate Polymers, 212*, 395–402.

Nishiyama, N., Kato, Y., Sugiyama, Y., & Kataoka, K. (2001). Cisplatin-loaded polymer-metal complex micelle with time-modulated decaying property as a novel drug delivery system. *Pharmaceutical Research, 18*, 1035–1041.

Ohta, S., Hiramoto, S., Amano, Y., Sato, M., Suzuki, Y., Shinohara, M., et al. (2016). Production of Cisplatin-Incorporating Hyaluronan Nanogels via Chelating Ligand-Metal Coordination. *Bioconjugate Chemistry, 27*, 504–508.

Ohta, S., Hiramoto, S., Amano, Y., Emoto, S., Yamaguchi, H., Ishigami, H., et al. (2017). Intraperitoneal delivery of cisplatin via a hyaluronan-based nanogel/*in Situ* cross-linkable hydrogel hybrid system for peritoneal dissemination of gastric cancer. *Molecular Pharmaceutics, 14*, 3105–3113.

Pan, N. C., Bersaneti, G. T., Mali, S., & Celligoi, M. A. P. C. (2020). Films based on blends of polyvinyl alcohol and microbial hyaluronic acid. *Brazilian Archives of Biology and Technology, 63*.

Rebenda, D., Vrbka, M., Čípek, P., Toropitsyn, E., Nečas, D., Pravda, M., et al. (2020). On the dependence of rheology of hyaluronic acid solutions and frictional behavior of articular cartilage. *Materials, 13*, 2659.

Riccio, B. V. F., Silvestre, A. L. P., Meneguin, A. B., Ribeiro, T. C., Klosowski, A. B., Ferrari, P. C., et al. (2022). Exploiting polymeric films as a multipurpose drug delivery system: a review. *AAPS PharmSciTech, 23*, 269.

Saravanakumar, G., Deepagan, V. G., Jayakumar, R., & Park, J. H. (2014). Hyaluronic acid-based conjugates for tumor-targeted drug delivery and imaging. *Journal of Biomedical Nanotechnology, 10*, 17–31.

Sheu, C., Shalumon, K. T., Chen, C. H., Kuo, C. Y., Fong, Y. T., & Chen, J. P. (2016). Dual crosslinked hyaluronic acid nanofibrous membranes for prolonged prevention of post-surgical peritoneal adhesion. *Journal of Materials Chemistry B, 4*, 6680–6693.

Sonvico, F., Barbieri, S., Colombo, P., Mucchino, C., Barocelli, E., Cantoni, A. M., et al. (2018). Physicochemical and pharmacokinetic properties of polymeric films loaded with cisplatin for the treatment of malignant pleural mesothelioma. *Journal of Thoracic Disease, 10*, S194–S206.

Talebian, S., Foroughi, J., Wade, S. J., Vine, K. L., Dolatshahi-Pirouz, A., Mehrali, M., et al. (2018). Biopolymers for antitumor implantable drug delivery systems: recent advances and future outlook. *Advanced Materials, 30*, Article e1706665.

Teresa, M., Laguna, R., Medrano, R., Plana, M. P., & Tarazona, M. P. (2001). Polymer characterization by size-exclusion chromatography with multiple detection. *Journal of Chromatography A, 919*, 13–19.

Tsai, S. W., Yu, D. S., Tsao, S. W., & Hsu, F. Y. (2013). Hyaluronan-cisplatin conjugate nanoparticles embedded in Eudragit S100-coated pectin/alginate microbeads for colon drug delivery. *International Journal of Nanomedicine, 8*, 2399–2407.

Wen, R., Umeano, A. C., Chen, P., & Farooqi, A. A. (2018). Polymer-based drug delivery systems for cancer. *Critical Reviews in Therapeutic Drug Carrier Systems, 35*, 521–553.

Xie, Y., Aillon, K. L., Cai, S., Christian, J. M., Davies, N. M., Berkland, C. J., et al. (2010). Pulmonary delivery of cisplatin-hyaluronan conjugates via endotracheal instillation for the treatment of lung cancer. *International Journal of Pharmaceutics, 392*, 156–163.

Yang, X., Salado-Leza, D., Porcel, E., González-Vargas, C. R., Savina, F., Dragoe, D., et al. (2020). A facile one-pot synthesis of versatile PEGylated platinum nanoflowers and their application in radiation therapy. *International Journal of Molecular Sciences, 21*, 1619.

Zhang, J. S., Anraku, M., Kadowaki, D., Imai, T., Suenaga, A., Odani, A., et al. (2011). Spectroscopic studies of interactions of chondroitin sulfates with cisplatin. *Carbohydrate Research, 346*, 631–637.